Effective property of multiferroic fibrous composites with imperfect interfaces

2013 Smart Mater. Struct. 22 105005

(http://iopscience.iop.org/0964-1726/22/10/105005)

Smart Mater. Struct. **22** (2013) 105005 (8pp) doi:10.1088/0964-1726/22/10/105005

Effective property of multiferroic fibrous composites with imperfect interfaces

Hsin-Yi Kuo

Department of Civil Engineering, National Chiao Tung University, Hsinchu 30010, Taiwan

E-mail: hykuo@mail.nctu.edu.tw

Received 11 April 2013, in final form 6 August 2013
Published 29 August 2013
Online at stacks.iop.org/SMS/22/105005

Abstract
This paper studies the effective behavior of piezoelectric and piezomagnetic circular fibrous composites with imperfect interfaces under longitudinal shear with in-plane electromagnetic fields. Two kinds of imperfect contact are investigated: mechanically stiff and dielectrically/magnetically highly conducting interfaces, and mechanically compliant and dielectrically/magnetically weakly conducting interfaces. For the former case, the potential field is continuous, while the normal component of the flux undergoes a discontinuity across the interface. For the latter case, the normal component of the flux is continuous, while there is a jump of potential field at such a contact. The classic work of Rayleigh (1892 *Phil. Mag.* **34** 481–502) in a periodic conductive perfect composite is generalized to the current coupled magnetoelectroelastic composites with imperfect interfaces. It is shown that the expression of the effective property has exactly the same form as that in the ideal coupling composite. Finally, this method is used to study $BaTiO_3$–$CoFe_2O_4$ composites and provide insights into enhancing the effective magnetoelectric voltage coefficient by properly choosing the interface.

(Some figures may appear in colour only in the online journal)

1. Introduction

Magnetoelectricity (ME) in multiferroic composites, which is related to inducing an electric polarization by a magnetic field or conversely inducing a magnetization by an electric field, has been the topic of a number of theoretical and experimental investigations in recent years. The coupling between the electric and magnetic fields provides opportunities for technological applications in sensing, actuation, and data storage (Fiebig 2005, Ramesh and Spaldin 2007, Kumar *et al* 2009). A state of the art of recent development can be found in Eerenstein *et al* (2006), Nan *et al* (2008), and Bichurin *et al* (2010). The ME effect in the multiferroic composite is achieved through the product property: an applied magnetic field generates a strain in the ferromagnetic material, which in turn induces a strain in the ferroelectric material, resulting in a polarization. Each phase possesses either magnetostrictive or piezoelectric properties, and the product ME effect is a new property determined by the mechanical interaction between the two phases. Therefore, the interface is critical in achieving the giant magnetoelectricity.

In earlier investigation the interface between the ferroelectric and ferromagnetic constituents was primarily assumed to be perfect or ideal coupling (see, for instance, Harshé *et al* 1993, Nan 1994, Benveniste 1995, Li and Dunn 1998, Liu and Kuo 2012, Kuo and Bhattacharya 2013). However, measured ME coupling coefficients may be notably discrepant with the above theories for both the ME particulate composites and laminates. To explain the discrepancies, an interface coupling parameter that defines the degree to which the deformation of the piezoelectric layer follows that of the magnetostrictive layer was introduced by Bichurin *et al* (2003). Nan *et al* (2003) studied the influence of the interfacial bonding on the ME effect in the multiferroic PZT–Terfenol-D laminated composite by means of the Green's function approach. Chang and Carman (2007) proposed a quasistatic theoretical model including shear lag and demagnetization effect for predicting the ME effects in an ME laminate. Wang and Pan (2007) used the complex variable approach together with the Mori–Tanaka mean field method to derive the effective moduli of multiferroic fibrous composites. All the above studies were primarily concerned

with the soft interface at which different tangential strains or electromagnetic fields may occur. On the other hand, owing to the minimization of components, the surface elasticity theory, which describes the membrane-type stiff interface, has been recently developed to account for the effects of surfaces and interfaces at nanoscales (Benveniste and Miloh 2001, Sharma *et al* 2003, Chen *et al* 2007). Pan *et al* (2009) generalized this idea to the field of the multiferroic fibrous nanocomposite with a size effect along its interface.

For the general problem of a transversely isotropic multiferroic composite, Benveniste (1995) has shown that it can be decomposed into two independent problems, plane strain with transverse electromagnetic fields and anti-plane shear with in-plane electromagnetic field. The anti-plane shear deformation therefore serves as part of the contribution that is present in a three-dimensional situation. Further, this out-of-plane deformation mode has wide applications in screw dislocation, in which the slip vector is parallel to the dislocation line (Zheng *et al* 2007), and Mode III crack problems, in which a shear stress acting parallel to the plane of the crack and parallel to the crack front (Spyropoulos *et al* 2003, Wang and Mai 2004, Gao *et al* 2004, Hao and Liu 2006, Guo and Lu 2010).

Motivated by these advances, and in a departure from previous work, this paper develops a new formulation to study the effective behavior of multiferroic fibrous composites with imperfect interfaces under longitudinal shear with in-plane electromagnetic fields. Both the fiber and matrix are assumed to be transversely isotropic. Two kinds of imperfect interface are considered: (i) mechanically stiff and electromagnetically highly conducting, which is a generalization of a membrane-type interface, and (ii) mechanically compliant and electromagnetically weakly conducting, which is a general extension of the shear lag model. For the former case, the potentials (displacement, electric potential and magnetic potential) are continuous across the interface, while the normal component of flux (stress, electric displacement, and magnetic flux) undergoes a discontinuity which is proportional to the local surface Laplacian of the potential field. For the latter case, the normal fluxes are continuous, while the potentials are discontinuous at such contact. The jumps in potential components are further assumed to be proportional to their respective interface flux components. These general imperfect contacts could model various types of interfacial damage such as debonding, sliding, cracking, or surface effects across the interface.

This paper is organized as follows. In section 2 the basic formulation is introduced for a composite medium made of piezoelectric and piezomagnetic phases arranged in a microstructure consisting of parallel cylinders in a matrix subjected to anti-plane shear deformation and in-plane electromagnetic fields. Following Kuo and Bhattacharya (2013), each field in each medium is expanded in a series in section 3. Two kinds of imperfect contact are studied: mechanically stiff and dielectrically/magnetically highly conducting interfaces, and mechanically compliant and dielectrically/magnetically weakly conducting interfaces. Expressions for effective properties are obtained in section 4. Numerical results are shown in section 5 using composites of $BaTiO_3$ and $CoFe_2O_4$. It is shown that the effective ME effect can be substantially enhanced by properly choosing the interface, providing an opportunity for controlling the ME effect and other effective moduli of the composites.

2. Formulation

Consider a composite consisting of a periodic array of parallel and separated prismatic circular cylinders with radius a. Assume that the cylinders and the matrix are made of distinct phases: transversely isotropic piezoelectric or piezomagnetic materials. A Cartesian coordinate system is introduced with the xy-axes in the plane of the cross-section and the z-axis along the axes of the cylinders.

Now assume that the composite is subjected to anti-plane shear strains $\bar{\varepsilon}_{zx}, \bar{\varepsilon}_{zy}$, in-plane electric fields $\bar{E}_x, \bar{E}_y$ and magnetic fields $\bar{H}_x, \bar{H}_y$ at infinity. Thus the composite is in a state of generalized anti-plane shear deformation and can be described by Benveniste (1995)

$$\begin{aligned} u_x = u_y = 0, \qquad u_z = w(x,y), \\ \varphi = \varphi(x,y), \\ \psi = \psi(x,y), \end{aligned} \tag{2.1}$$

where u_x, u_y, and u_z are the mechanical displacements along the x-, y-, and z-axes, and φ and ψ are the electric and magnetic potentials, respectively.

The constitutive laws of the kth phase for the non-vanishing fields can be recast in the compact form as

$$\mathbf{\Sigma}_j^{(k)} = \mathbf{L}^{(k)}\mathbf{Z}_j^{(k)}, \qquad j = x, y, \tag{2.2}$$

where for ease of terminology $k =$ 'm' ($k =$ 'i') refers to the matrix (inclusion) phase,

$$\begin{aligned} \mathbf{\Sigma}_j^{(k)} &= \begin{pmatrix} \sigma_{zj} \\ D_j \\ B_j \end{pmatrix}^{(k)}, \\ \mathbf{L}^{(k)} &= \begin{pmatrix} C_{44} & e_{15} & q_{15} \\ e_{15} & -\kappa_{11} & -\lambda_{11} \\ q_{15} & -\lambda_{11} & -\mu_{11} \end{pmatrix}^{(k)}, \\ \mathbf{Z}_j^{(k)} &= \begin{pmatrix} \varepsilon_{zj} \\ -E_j \\ -H_j \end{pmatrix}^{(k)}. \end{aligned} \tag{2.3}$$

In equations (2.3), σ_{zj} and ε_{zj} are the shear stress and strain; D_j and E_j are the electric displacement and electric field vectors; B_j and H_j are the magnetic flux and magnetic field vectors. The material constants $C_{44}, \kappa_{11}, \mu_{11}$, and λ_{11} are the elastic modulus, dielectric permittivity, magnetic permeability, and magnetoelectric coefficient, while e_{15} and q_{15} are the piezoelectric and piezomagnetic coefficients.

The shear strains ε_{zx} and ε_{zy}, in-plane dielectric fields E_x and E_y, and in-plane magnetic fields H_x and H_y can be derived

from the gradient of elastic displacement w, electric potential φ, and magnetic potential ψ as follows:

$$\mathbf{Z}_j = \mathbf{\Phi}_{,j} = \begin{pmatrix} w_{,j} \\ \varphi_{,j} \\ \psi_{,j} \end{pmatrix}. \tag{2.4}$$

Here the subscript j following a comma denotes the derivative with respect to x or y. In the absence of body force, electric charge density, and electric current density, the equilibrium equations are given by

$$\mathbf{L}\nabla^2\mathbf{\Phi} = \mathbf{0}, \tag{2.5}$$

where $\nabla^2 = \partial^2/\partial x^2 + \partial^2/\partial y^2$ is the two-dimensional Laplace operator for the variables x and y. Since $\mathbf{L}$ is a nonsingular matrix, equation (2.5) can be decoupled into three independent Laplace equations,

$$\nabla^2\mathbf{\Phi} = \mathbf{0}, \tag{2.6}$$

in the interior of each phase. In other words, the three fields—displacement, electrostatic potential and magnetostatic potential—are completely decoupled in the interior of each phase.

3. Circular cylinders with imperfect interfaces

Consider a situation where the composite is subjected to a macroscopically uniaxial loading along the positive x-axis

$$\mathbf{\Phi}_{\text{ext}} = \bar{\mathbf{Z}}_x x, \tag{3.1}$$

where $\bar{\mathbf{Z}}_x = (\bar{\varepsilon}_{zx}, -\bar{E}_x, -\bar{H}_x)^t$. Under the above generalized anti-plane shear deformation, the potential field for the circular cylinder and its surrounding matrix can be expanded with respect to its center O in polar coordinates (r, θ) as (Kuo and Bhattacharya 2013)

$$\mathbf{\Phi}^{(m)}(\mathbf{x}) = \mathbf{a}_0 + \sum_{n=1}^{\infty}(\mathbf{a}_n r^n + \mathbf{b}_n r^{-n})\cos n\theta \tag{3.2}$$

for the matrix, and

$$\mathbf{\Phi}^{(i)}(\mathbf{x}) = \mathbf{c}_0 + \sum_{n=1}^{\infty}\mathbf{c}_n r^n \cos n\theta \tag{3.3}$$

for the inclusion, where

$$\mathbf{a}_n = \begin{pmatrix} A_n^w \\ A_n^\varphi \\ A_n^\psi \end{pmatrix}, \qquad \mathbf{b}_n = \begin{pmatrix} B_n^w \\ B_n^\varphi \\ B_n^\psi \end{pmatrix}, \qquad \mathbf{c}_n = \begin{pmatrix} C_n^w \\ C_n^\varphi \\ C_n^\psi \end{pmatrix}. \tag{3.4}$$

The coefficients $\mathbf{a}_n, \mathbf{b}_n$, and $\mathbf{c}_n$ are unknown constants to be determined from the interface and boundary conditions. Note that the sine terms that would be present in a general expansion are missing since a uniaxial loading along the x-direction is imposed.

In order to treat the imperfect interface effect, we first resort to a more general three-phase composite of a similar distribution in which the inclusions possess a concentric elastic coating of thickness t and material parameter $\mathbf{L}_c = \text{diag}(C_{44}, -\kappa_{11}, -\mu_{11})$ (Torquato and Rintoul 1995, Hashin 2001, Miloh and Benveniste 1999). By passing to the limit where $t \to 0$ and either $\mathbf{L}_c^{-1} \to \mathbf{0}$ (mechanically stiff and dielectrically/magnetically highly conducting interface) or $\mathbf{L}_c \to \mathbf{0}$ (mechanically soft and dielectrically/magnetically weakly conducting interface), we recover the distribution of interest in which the interfacial property is characterized by the parameters $\boldsymbol{\alpha}$ and $\boldsymbol{\beta}$ given by

$$\boldsymbol{\alpha} = \lim_{\substack{t\to 0 \\ \mathbf{L}_c^{-1}\to\mathbf{0}}} (\mathbf{L}_c t) = \begin{pmatrix} \alpha^w & 0 & 0 \\ 0 & \alpha^\varphi & 0 \\ 0 & 0 & \alpha^\psi \end{pmatrix} \tag{3.5}$$

for the mechanically stiff and dielectrically/magnetically highly conducting case, and

$$\boldsymbol{\beta} = \lim_{\substack{t\to 0 \\ \mathbf{L}_c\to\mathbf{0}}} (\mathbf{L}_c / t) = \begin{pmatrix} \beta^w & 0 & 0 \\ 0 & \beta^\varphi & 0 \\ 0 & 0 & \beta^\psi \end{pmatrix} \tag{3.6}$$

for the mechanically soft and dielectrically/magnetically weakly conducting case.

Now consider that the interface is mechanically stiff and dielectrically/magnetically highly conducting. It has been shown that in this case, with $\boldsymbol{\alpha}$ given by (3.5), the potential $\mathbf{\Phi}$ is continuous across the interface ∂V, while there is a jump in the normal component of the current (Miloh and Benveniste 1999, Pan *et al* 2009). Specifically, one has

$$\begin{aligned} \mathbf{\Sigma}_j^{(m)} n_j|_{\partial V} - \mathbf{\Sigma}_j^{(i)} n_j|_{\partial V} &= \boldsymbol{\alpha}\nabla_s^2 \mathbf{\Phi}^{(i)}|_{\partial V}, \\ \mathbf{\Phi}^{(m)}|_{\partial V} &= \mathbf{\Phi}^{(i)}|_{\partial V}, \end{aligned} \tag{3.7}$$

where $\nabla_s^2 = \frac{1}{r^2}\frac{\partial^2}{\partial\theta^2}$ is the surface Laplace operator, $\mathbf{n}$ is the unit outward normal to the interface ∂V: $r = a$, and the repeated index j denotes the summation over the components x and y. The case where $\boldsymbol{\alpha} = \mathbf{0}$ corresponds to a perfect interface, whereas $\boldsymbol{\alpha}^{-1} = \mathbf{0}$ describes an isoexpansion and equipotential interface.

Using the orthogonality properties of trigonometric functions, the interface conditions (3.7) provide

$$\begin{aligned} \mathbf{a}_n &= a^{-2n}\mathbf{T}_n\mathbf{b}_n, \\ \mathbf{c}_n &= a^{-2n}(\mathbf{T}_n + \mathbf{I})\mathbf{b}_n, \qquad n \geq 1, \end{aligned} \tag{3.8}$$

and $\mathbf{a}_0 = \mathbf{c}_0$, where $\mathbf{a}_n$, $\mathbf{b}_n$, $\mathbf{c}_n$ are defined in (3.4), $\mathbf{I}$ is the 3×3 identity tensor, and

$$\mathbf{T}_n = (\mathbf{L}^{(m)} - \mathbf{L}^{(i)} + \mathbf{\Lambda}_n)^{-1}(\mathbf{L}^{(m)} + \mathbf{L}^{(i)} - \mathbf{\Lambda}_n), \tag{3.9}$$

$$\mathbf{\Lambda}_n = a^{-1} n\boldsymbol{\alpha}. \tag{3.10}$$

When $\boldsymbol{\alpha} = \mathbf{0}$, the results reduce to the perfectly bonded case (Kuo and Bhattacharya 2013).

Next, consider the interface is mechanically soft and dielectrically/magnetically weakly conducting with interfacial imperfection matrix $\boldsymbol{\beta}$ given by (3.6). It can be shown that in

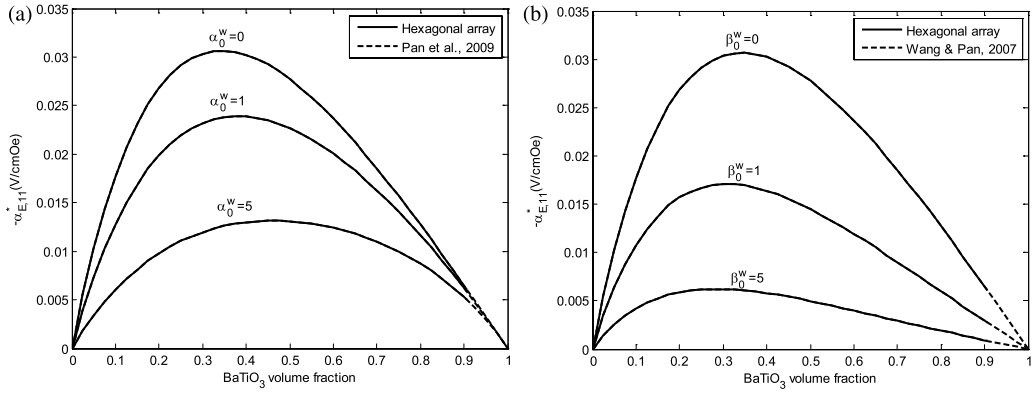

Figure 1. The predicted ME voltage coefficients for composites of $BaTiO_3$ fibers in a $CoFe_2O_4$ matrix: (a) mechanically stiff imperfect interfaces characterized by $\alpha^w = \alpha_0^w a C_{44}^{(i)}, \alpha^\varphi = 0, \alpha^\psi = 0$ and (b) mechanically soft imperfect interfaces characterized by $\beta^w = \beta_0^w a/C_{44}^{(i)}, \beta^\varphi = 0, \beta^\psi = 0$. Here α_0^w and β_0^w are dimensionless parameters. In both (a) and (b), the solid line '–' is based on the presented solution for a hexagonal array. The dashed line '- -' is from Pan *et al* (2009) for (a) and is from Wang and Pan (2007) for (b).

this case the potential $\mathbf{\Phi}$ has a jump on the interface boundary ∂V, which is proportional to the normal component $\mathbf{\Sigma}_j n_j$ of the current, which is continuous across the interface (Miloh and Benveniste 1999, Wang and Pan 2007),

$$\begin{aligned} \mathbf{\Sigma}_j^{(m)} n_j|_{\partial V} &= \mathbf{\Sigma}_j^{(i)} n_j|_{\partial V}, \\ \mathbf{\Phi}^{(m)}|_{\partial V} - \mathbf{\Phi}^{(i)}|_{\partial V} &= \boldsymbol{\beta}\mathbf{\Sigma}_j^{(i)} n_j|_{\partial V}. \end{aligned} \tag{3.11}$$

The case where $\boldsymbol{\beta} = \mathbf{0}$ corresponds to a perfectly bonded interface, whereas $\boldsymbol{\beta}^{-1} = \mathbf{0}$ describes a completely debonded and electric charge-free (insulating) interface.

Analogous to (3.8), the interface conditions (3.11) give constraints

$$\begin{aligned} &\mathbf{a}_n = a^{-2n}\mathbf{T}_n\mathbf{b}_n, \\ &\mathbf{c}_n = a^{-2n}[(\mathbf{I} - \mathbf{\Pi}_n)\mathbf{T}_n + \mathbf{I} + \mathbf{\Pi}_n]\mathbf{b}_n, \qquad n \geq 1, \end{aligned} \tag{3.12}$$

and $\mathbf{a}_0 = \mathbf{c}_0$, where $\mathbf{a}_n$, $\mathbf{b}_n$, $\mathbf{c}_n$ are defined in (3.4), and

$$\mathbf{T}_n = (\mathbf{L}^{(m)} - \mathbf{L}^{(i)} + \mathbf{\Lambda}_n)^{-1}(\mathbf{L}^{(m)} + \mathbf{L}^{(i)} + \mathbf{\Lambda}_n), \tag{3.13}$$

$$\mathbf{\Lambda}_n = a^{-1} n \mathbf{L}^{(i)} \boldsymbol{\beta} L^{(m)}, \qquad \mathbf{\Pi}_n = a^{-1} n \boldsymbol{\beta} L^{(m)}. \tag{3.14}$$

Again, when $\boldsymbol{\beta} = \mathbf{0}$, the equation recovers the previous results of the ideal coupling contact.

Finally, imposing the periodicity conditions yields a generalized Rayleigh identity

$$\mathbf{a}_n + \sum_{m=1}^{\infty} \binom{m+n-1}{n} S_{m+n}\mathbf{b}_m = \bar{\mathbf{Z}}_x \delta_{n,1}, \tag{3.15}$$

where $\delta_{n,1}$ is the Kronecker delta, and the quantities

$$S_m = \sum_{l \neq O} \mathrm{Re}(X_l + \mathrm{i}Y_l)^{-m} \tag{3.16}$$

are the lattice sums characterizing the geometry of the periodic structure, and $X_l + \mathrm{i}Y_l$ is the center of the lth cylinder when measured at the central point O. The index l runs over all cylinders' centers underlying the periodic array except the central one. A list of non-zero normalized lattice sums for square and hexagonal arrays can be found in Berman and Greengard (1994).

Equations (3.15) and $(3.8)_1$ or $(3.12)_1$ constitute an infinite set of linear algebraic equations. Upon appropriate truncations of the expansion terms at some finite order $m = M$, the expansion coefficients $\mathbf{a}_n$, $\mathbf{b}_n$, and $\mathbf{c}_n$ can be determined.

4. Effective moduli

Now we turn to obtain the effective moduli of the composite from the solution of (3.15). The major distinction from previous studies is that the inclusions have interfacial imperfections. The effective material properties are defined in terms of average fields,

$$\langle \mathbf{\Sigma}_j \rangle \equiv \mathbf{L}^* \langle \mathbf{Z}_j \rangle, \tag{4.1}$$

where the angular brackets denote the average over the representative volume element V (or unit cell in the periodic case), i.e.,

$$\langle \mathbf{\Sigma}_j \rangle = \frac{1}{V}\int_V \mathbf{\Sigma}_j \, \mathrm{d}V, \qquad \langle \mathbf{Z}_j \rangle = \frac{1}{V}\int_V \mathbf{Z}_j \, \mathrm{d}V, \tag{4.2}$$

and $\mathbf{L}^*$ denotes the effective magnetoelectroelastic parameters of the composite.

When (3.1) is prescribed, statistical homogeneity in the fields $\mathbf{Z}_x$ simply implies

$$\langle \mathbf{Z}_x \rangle = \bar{\mathbf{Z}}_x. \tag{4.3}$$

For a mechanically stiff and dielectrically/magnetically highly conducting interface, the average flux, $\langle \mathbf{\Sigma}_x \rangle$, is now given by Miloh and Benveniste (1999)

$$\begin{aligned} \langle \mathbf{\Sigma}_x \rangle = \frac{1}{V}\Bigg[&\int_{V_m} \mathbf{\Sigma}_x^{(m)} \, \mathrm{d}V + \int_{V_i} \mathbf{\Sigma}_x^{(i)} \, \mathrm{d}V \\ &+ \int_{\partial V} (\mathbf{\Sigma}_j^{(m)} - \mathbf{\Sigma}_j^{(i)}) n_j x \, \mathrm{d}s\Bigg], \end{aligned} \tag{4.4}$$

which contains an additional integral involving the normal flux jump across the interface ∂V. Substituting $(3.7)_1$, $(4.2)_2$, (4.3), and the constitutive relation (2.2) into the above

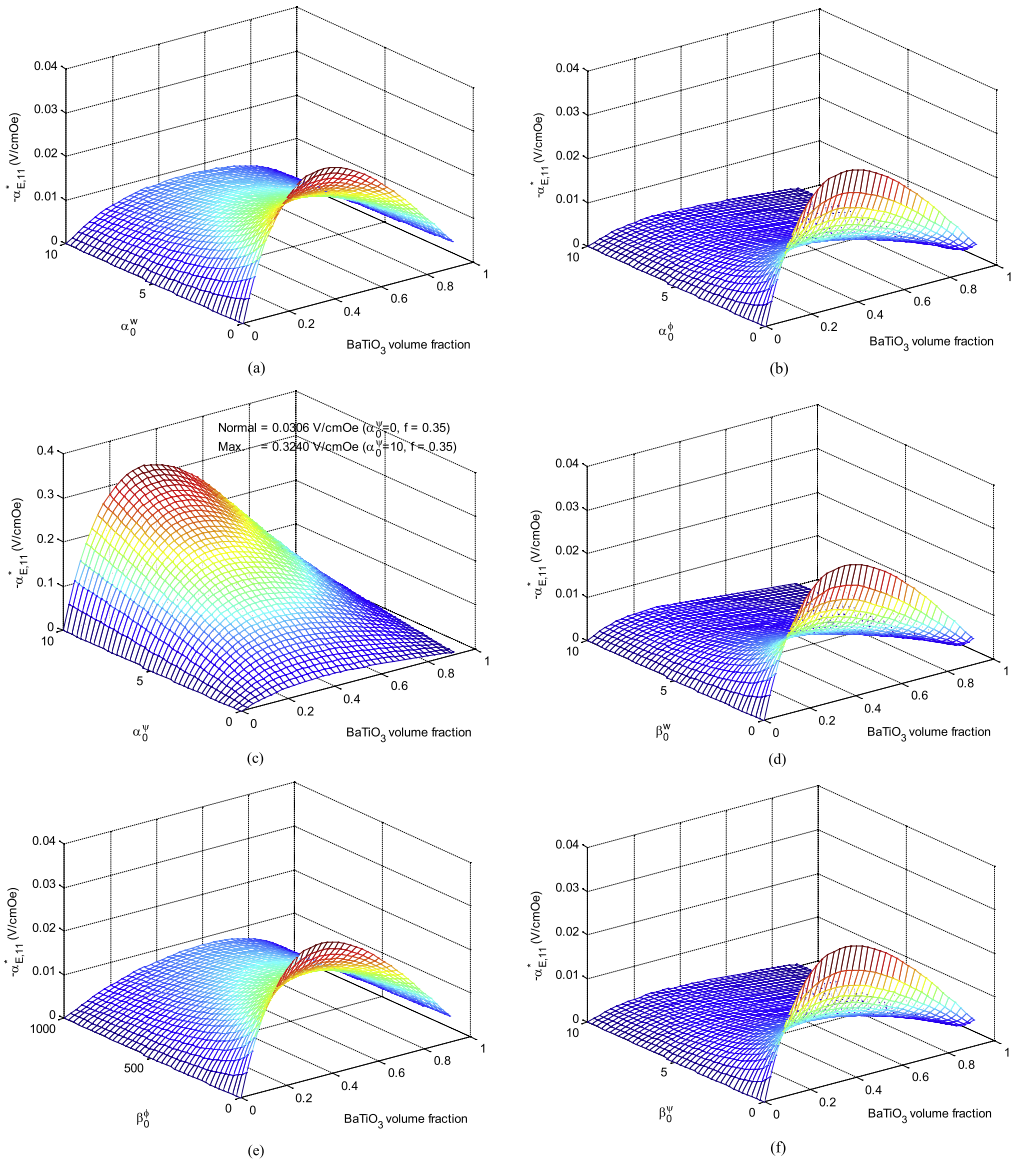

Figure 2. The contour plots of the ME voltage coefficient $\alpha^*_{E,11}$ versus $BaTiO_3$ volume fraction and different interface parameters for a composite of $BaTiO_3$ fibers in a $CoFe_2O_4$ matrix. The interface imperfections include (a) mechanically stiff interface ($\alpha^w = \alpha_0^w aC_{44}^{(i)}, \alpha^\varphi = 0, \alpha^\psi = 0$), (b) electrically highly conducting interface ($\alpha^w = 0, \alpha^\varphi = -\alpha_0^\varphi a\kappa_{11}^{(i)}, \alpha^\psi = 0$), (c) magnetically highly conducting interface ($\alpha^w = 0, \alpha^\varphi = 0, \alpha^\psi = -\alpha_0^\psi a\mu_{11}^{(i)}$), (d) mechanically compliant interface ($\beta^w = \beta_0^w a/C_{44}^{(i)}, \beta^\varphi = 0, \beta^\psi = 0$), (e) dielectrically weakly conducting interface ($\beta^w = 0, \beta^\varphi = -\beta_0^\varphi a/\kappa_{11}^{(i)}, \beta^\psi = 0$), and (f) magnetically weakly conducting interface ($\beta^w = 0, \beta^\varphi = 0, \beta^\psi = -\beta_0^\psi a/\mu_{11}^{(i)}$). Here $\alpha_0^w, \alpha_0^\varphi, \alpha_0^\psi, \beta_0^w, \beta_0^\varphi$, and β_0^ψ are dimensionless parameters.

equation yields

$$\langle \boldsymbol{\Sigma}_x \rangle = \mathbf{L}^{(m)} \left\{ \bar{\mathbf{Z}}_x - \frac{1}{V} (\mathbf{L}^{(m)})^{-1} \left[(\mathbf{L}^{(m)} - \mathbf{L}^{(i)}) \times \int_{\partial V} x \boldsymbol{\Phi}^{(i)}_{,r} \mathrm{d}s - \boldsymbol{\alpha} \int_{\partial V} \Delta_s \boldsymbol{\Phi}^{(i)} x \mathrm{d}s \right] \right\}. \quad (4.5)$$

Here the subscript r following a comma denotes the derivative with respect to the r variable. Using multipole expansions of the potential fields in the inclusion (3.3) and recalling the relation $(3.8)_2$, one obtains

$$\langle \boldsymbol{\Sigma}_x \rangle = \mathbf{L}^{(m)} (\bar{\mathbf{Z}}_x - 2a^{-2} f \mathbf{b}_1), \quad (4.6)$$

where f is the volume fraction of the inclusion defined as $f = \pi a^2/V$ for square arrays and is $f = \frac{2\pi}{\sqrt{3}} a^2/V$ for hexagonal arrays.

On the other hand, for a mechanically compliant and dielectrically/magnetically weakly conducting interface, the average intensity, $\langle \mathbf{Z}_x \rangle$, is now given by Benveniste and Miloh (1986)

$$\langle \mathbf{Z}_x \rangle = \frac{1}{V} \left[\int_{V_m} \boldsymbol{\Phi}^{(m)}_{,x} \, \mathrm{d}V + \int_{V_i} \boldsymbol{\Phi}^{(i)}_{,x} \, \mathrm{d}V + \int_{\partial V} (\boldsymbol{\Phi}^{(m)} - \boldsymbol{\Phi}^{(i)}) n_x \, \mathrm{d}s \right], \quad (4.7)$$

which contains an additional integral involving the potential jump across the interface ∂V. Substituting $(3.11)_2$, $(4.2)_2$, (4.3), and the constitutive laws (2.2) into $(4.2)_1$ yields

$$\langle \boldsymbol{\Sigma}_x \rangle = \mathbf{L}^{(m)} \left\{ \bar{\mathbf{Z}}_x - \frac{1}{V} \left[\boldsymbol{\beta}^{-1} \mathbf{L}^{(i)} \int_{\partial V} \boldsymbol{\Phi}^{(i)}_{,r} n_x \, \mathrm{d}s + (\mathbf{I} - (\mathbf{L}^{(m)})^{-1} \mathbf{L}^{(i)}) \int_{\partial V} x \boldsymbol{\Phi}^{(i)}_{,r} \, \mathrm{d}s \right] \right\}. \quad (4.8)$$

Making use of (3.3) and $(3.12)_2$, one obtains again (4.6).

Putting together (4.1) and (4.6) and noting that the coefficients $\mathbf{b}_1$ depend linearly on the applied field $\bar{\mathbf{Z}}_x$, a set of equations is then obtained for the effective property $\mathbf{L}^*$. By applying different loading combinations between $\bar{\varepsilon}_{zx}$, $\bar{E}_x$ and $\bar{H}_x$, all the components of $\mathbf{L}^*$ can be determined. Note that, although the inclusions now have imperfect interfaces, equation (4.6) has exactly the same form as that in the perfect case (Kuo and Bhattacharya 2013), but here the coefficients $\mathbf{b}_1$ incorporate the effect of the imperfect contact.

5. Results and discussion

The above framework is applied below to the $BaTiO_3$–$CoFe_2O_4$ (BTO–CFO) multiferroic composite, which has been studied by other researchers. The hexagonal array, and both BTO fibers in a CFO matrix and CFO fibers in a BTO matrix, are considered. The independent material constants of BTO are $C_{44} = 43 \times 10^9$ N m^{-2}, $e_{15} = 11.6$ C m^{-2}, $\kappa_{11} = 11.2 \times 10^{-9}$ C^2 N^{-1} m^{-2}, $\mu_{11} = 5 \times 10^{-6}$ N s^2 C^{-2}; while those of CFO are $C_{44} = 45.3 \times 10^9$ N m^{-2}, $q_{15} = 550$ N A^{-1} m^{-1}, $\kappa_{11} = 0.08 \times 10^{-9}$ C^2 N^{-1} m^{-2}, $\mu_{11} = 590 \times 10^{-6}$ N s^2 C^{-2} (Wang and Pan 2007). Here the xy-plane is the isotropic plane and the unique axis is along the z-direction. Note that in both materials ME coefficients are zero, i.e. $\lambda_{11} = 0$. A material property of particular interest is the ME voltage coefficient

$$\alpha^*_{E,11} = \lambda^*_{11}/\kappa^*_{11}, \quad (5.1)$$

where $\lambda^*_{11}(\kappa^*_{11})$ is the effective ME coefficient (dielectric permittivity) of the composite. It relates to the overall electric field that is generated in the composite when it is subjected to a magnetic field and is the figure of merit for magnetic field sensors.

To check the correctness of the formulation, the ME voltage coefficients for a composite of BTO fibers in a CFO matrix is studied first. Figure 1 shows how the ME voltage coefficient depends on the BTO volume fraction and different mechanical interfacial imperfections. The order of truncation is $M = 4$. Figure 1(a) is for mechanically stiff imperfect interfaces characterized by $\alpha^w = \alpha^w_0 a C^{(i)}_{44}$ and $\alpha^\varphi = 0, \alpha^\psi = 0$ while figure 1(b) is for mechanically soft imperfect interfaces characterized by $\beta^w = \beta^w_0 a / C^{(i)}_{44}$ and $\beta^\varphi = 0, \beta^\psi = 0$. Here α^w_0 and β^w_0 are dimensionless parameters. The curves vary nonlinearly with volume fraction, and they stop around $f = \pi/(2\sqrt{3})$ when the inclusions begin to touch each other for hexagonal arrays. The ME voltage coefficient decreases as α^w_0 (β^w_0) increases. For comparisons, figure 1 also plots the effective moduli with those predicted by Pan *et al* (2009) (for the mechanically stiff case) and Wang and Pan (2007) (for the mechanically soft case) who used the complex variable approach and the Mori–Tanaka method. In the Mori–Tanaka method, there is no upper limit on the volume fractions. Still, the overall magnitudes and trends agree well between the present periodic and their Mori–Tanaka method.

Figure 2 shows the ME voltage coefficient for a composite of BTO fibers in a CFO matrix as a function of inclusion volume fraction for different interfacial imperfections: (a) mechanically stiff interface ($\alpha^w = \alpha^w_0 a C^{(i)}_{44}, \alpha^\varphi = 0, \alpha^\psi = 0$), (b) electrically highly conducting interface ($\alpha^w = 0, \alpha^\varphi = -\alpha^\varphi_0 a \kappa^{(i)}_{11}, \alpha^\psi = 0$), (c) magnetically highly conducting interface ($\alpha^w = 0, \alpha^\varphi = 0, \alpha^\psi = -\alpha^\psi_0 a \mu^{(i)}_{11}$), (d) mechanically soft interface ($\beta^w = \beta^w_0 a / C^{(i)}_{44}, \beta^\varphi = 0, \beta^\psi = 0$), (e) dielectrically weakly conducting interface ($\beta^w = 0, \beta^\varphi = -\beta^\varphi_0 a / \kappa^{(i)}_{11}, \beta^\psi = 0$), (f) magnetically weakly conducting interface ($\beta^w = 0, \beta^\varphi = 0, \beta^\psi = -\beta^\psi_0 a / \mu^{(i)}_{11}$). Here $\alpha^w_0, \alpha^\varphi_0, \alpha^\psi_0, \beta^w_0, \beta^\varphi_0$, and β^ψ_0 are dimensionless parameters. It is observed that except for the magnetically highly conducting interface (figure 2(c)), all the coupling constants are reduced as compared to that for a perfect case. The ME voltage constant in figure 2(c) is substantially enhanced as α^ψ_0 increases. When α^ψ_0 changes from 0 to 10, the maximum value of 0.3240 V cm^{-1} Oe^{-1} at $f = 0.35$ is ten times higher than 0.0306 V cm^{-1} Oe^{-1} ($f = 0.35$), which is the optimal value of the perfectly bonded case. Further, the optimal value of the BTO volume fraction, at which the maximum ME voltage coefficients occurs, basically remains the same as α^ψ_0 increases. Because $\alpha^\psi = -\alpha^\psi_0 a \kappa^{(i)}_{11}$ is size dependent, this provides an excellent chance for enhancing the ME effect in nanocomposites using the size-dependent feature.

Now turn to the composite of CFO fibers in a BTO matrix. Figure 3 shows the ME voltage coefficient as a function of inclusion volume fraction for different interfacial imperfections, and is the counterpart of figure 2. Similarly, in most cases ((a), (c)–(f)) the ME coupling coefficient is reduced as compared to that for a perfect contact. However, for the composite with electrically highly conducting interface (figure 3(b)), the ME effect is substantially enhanced as α^φ_0 increases. When α^φ_0 changes from 0 to 100, the maximum value of 0.0842 V cm^{-1} Oe^{-1} at $f = 0.90$ is around 7.39 times higher than 0.0114 V cm^{-1} Oe^{-1} ($f = 0.9069$), which is the optimal value of the perfectly bonded contact. In addition, the optimal value of the CFO volume fraction, at which the maximum ME voltage coefficients occurs, decreases as α^φ_0 increases. This also provides an alternative way to enhance the magnetoelectricity.

Note that the numerical results above show that, for a BTO–CFO composite, the mechanically compliant and dielectrically/magnetically weakly conducting interface all causes a decrease in the ME coupling.

6. Conclusions

A framework based on Rayleigh's formalism is developed for predicting the field distributions and effective properties

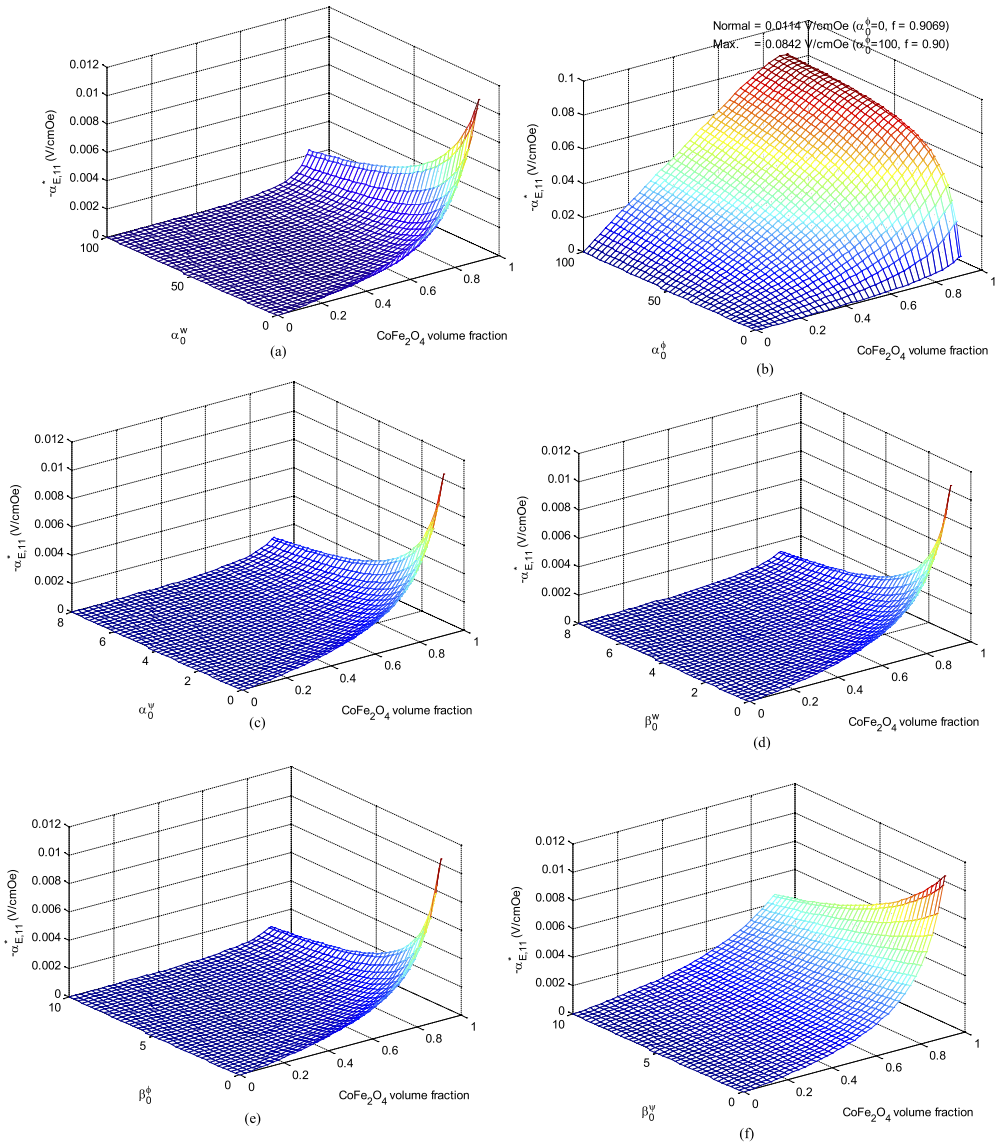

Figure 3. The contour plots of the ME voltage coefficient $\alpha^*_{E,11}$ versus $CoFe_2O_4$ volume fraction and different interface parameters for a composite of $CoFe_2O_4$ fibers in a $BaTiO_3$ matrix. The interface imperfections include (a) mechanically stiff interface ($\alpha^w = \alpha_0^w aC_{44}^{(i)}$, $\alpha^{\varphi} = 0$, $\alpha^{\psi} = 0$), (b) electrically highly conducting interface ($\alpha^w = 0$, $\alpha^{\varphi} = -\alpha_0^{\varphi} a\kappa_{11}^{(i)}$, $\alpha^{\psi} = 0$), (c) magnetically highly conducting interface ($\alpha^w = 0$, $\alpha^{\varphi} = 0$, $\alpha^{\psi} = -\alpha_0^{\psi} a\mu_{11}^{(i)}$), (d) mechanically compliant interface ($\beta^w = \beta_0^w a/C_{44}^{(i)}$, $\beta^{\varphi} = 0$, $\beta^{\psi} = 0$), (e) dielectrically weakly conducting interface ($\beta^w = 0$, $\beta^{\varphi} = -\beta_0^{\varphi} a/\kappa_{11}^{(i)}$, $\beta^{\psi} = 0$), and (f) magnetically weakly conducting interface ($\beta^w = 0$, $\beta^{\varphi} = 0$, $\beta^{\psi} = -\beta_0^{\psi} a/\mu_{11}^{(i)}$). Here α_0^w, α_0^{φ}, α_0^{ψ}, β_0^w, β_0^{φ}, and β_0^{ψ} are dimensionless parameters.

of the multiferroic composite consisting of regular arrays of circular cylinders with imperfect interfaces under generalized anti-plane shear deformation. Both mechanically stiff and dielectrically/magnetically highly conducting interfaces, and mechanically compliant and dielectrically/magnetically weakly conducting interfaces, are considered. Expressions for the elastic, electric, and magnetic potentials for the cylinders and the matrix are derived, and used to compute the macroscopic behavior. It is shown that the effective properties solely depend on one set of particular constants $\mathbf{b}_1$, and the formula of the effective property has exactly the same form as that in the perfectly bonded interface, although now the inclusions are with interfacial imperfection. Finally, as a practical example, the ME effects in $BaTiO_3$–$CoFe_2O_4$ composites are presented and discussed. This example shows the important difference between two kinds of imperfect contact. The present theoretical framework provides a general guideline and an alternative way for enhancing the magnetoelectricity.

Acknowledgments

The financial support from the National Science Council under grant NSC 100-2628-E-009-022-MY2 is gratefully acknowledged. The author is also grateful to anonymous reviewers for their helpful comments and suggestions.

References

Benveniste Y 1995 Magnetoelectric effect in fibrous composites with piezoelectric and piezomagnetic phases *Phys. Rev.* B **51** 16424–7

Benveniste Y and Miloh T 1986 The effective conductivity of composites with imperfect thermal contact at constituent interfaces *Int. J. Eng. Sci.* **24** 1537–52

Benveniste Y and Miloh T 2001 Imperfect soft and stiff interfaces in two-dimensional elasticity *Mech. Mater.* **33** 309–23

Berman C L and Greengard L 1994 A renormalization method for the evaluation of lattice sums *J. Math. Phys.* **35** 6036–48

Bichurin M I, Petrov V M, Averkin S V and Liverts E 2010 Present status of theoretical modeling the magnetoelectric effect in magnetostrictive–piezoelectric nanostructures. Part I: low frequency and electromechanical resonance ranges *J. Appl. Phys.* **107** 053904

Bichurin M I, Petrov V M and Srinivasan G 2003 Theory of low-frequency magnetoelectric coupling in magnetostrictive–piezoelectric bilayers *Phys. Rev.* B **68** 054402

Chang C-M and Carman G P 2007 Modeling shear lag and demagnetization effects in magneto-electric laminate composites *Phy. Rev.* B **76** 134116

Chen T, Dvorak G J and Yu C C 2007 Size-dependent elastic properties of unidirectional nano-composites with interface stresses *Acta Mech.* **188** 39–54

Eerenstein W, Mathur N D and Scott J F 2006 Multiferroic and magnetoelectric materials *Nature* **442** 759–65

Fiebig M 2005 Revival of the magnetoelectric effect *J. Phys. D: Appl. Phys.* **38** R123–52

Gao C-F, Tong P and Zhang T-Y 2004 Fracture mechanics for a mode III crack in a magnetoelectroelastic solid *Int. J. Solids Struct.* **41** 6613–29

Guo J-H and Lu Z-X 2010 Anti-plane analysis of multiple cracks originating from a circular hole in a magnetoelectroelastic solid *Int. J. Solids Struct.* **47** 1847–56

Hao R J and Liu J X 2006 Interaction of a screw dislocation with a semi-infinite interfacial crack in a magneto-electro-elastic bi-material *Mech. Res. Commun.* **33** 415–24

Harshé G, Dougherty J P and Newham R E 1993 Theoretical modelling of multilayer magnetoelectric composites *Int. J. Appl. Electromagn. Mater.* **4** 145–59

Hashin Z 2001 Thin interphase/imperfect interface in conduction *J. Appl. Phys.* **89** 2261–7

Kumar A, Sharma G L, Katiyar R S, Pirc R, Blinc R and Scott J F 2009 Magnetic control of ferroelectric polarization *J. Phys.: Condens. Matter* **21** 382204

Kuo H-Y and Bhattacharya K 2013 Fibrous composites of piezoelectric and piezomagnetic phases *Mech. Mater.* **60** 159–70

Li J Y and Dunn M L 1998 Micromechanics of magnetoelectroelastic composite materials: average fields and effective behavior *J. Intell. Mater. Syst. Struct.* **9** 404–16

Liu L P and Kuo H-Y 2012 Closed-form solutions to the effective properties of fibrous magnetoelectric composites and their applications *Int. J. Solids Struct.* **49** 3055–62

Miloh T and Benveniste Y 1999 On the effective conductivity of composites with ellipsoidal inhomogeneities and highly conducting interfaces *Proc. R. Soc.* A **455** 2687–706

Nan C-W 1994 Magnetoelectric effect in composites of piezoelectric and piezomagnetic phases *Phys. Rev.* B **50** 6082–8

Nan C-W, Bichurin M I, Dong S, Viehland D and Srinivasan G 2008 Multiferroic magnetoelectric composites: historical perspective, status and future directions *J. Appl. Phys.* **103** 031101

Nan C-W, Liu G and Lin Y 2003 Influence of interfacial bonding on giant magnetoelectric response of multiferroic laminated composites of $Tb_{1-x}Dy_xFe_2$ and $PbZr_xTi_{1-x}O_3$ *Appl. Phys. Lett.* **83** 4366–8

Pan E, Wang X and Wang R 2009 Enhancement of magnetoelectric effect in multiferroic fibrous nancomposites via size-dependent material properties *Appl. Phys. Lett.* **95** 181904

Ramesh R and Spaldin N A 2007 Multiferroics: progress and prospects in thin films *Nature Mater.* **6** 21–9

Sharma P, Ganti S and Bhate N 2003 Effect of surfaces on the size-dependent elastic state of nano-inhomogeneities *Appl. Phys. Lett.* **82** 535–7

Spyropoulos C P, Sih G C and Song Z F 2003 Magnetoelectroelastic composite with poling parallel to plane of line crack under out-of-plane deformation *Theor. Appl. Fract. Mech.* **39** 281–9

Torquato S and Rintoul M D 1995 Effect of the interface on the properties of composite media *Phys. Rev. Lett.* **75** 4067–70

Wang B-L and Mai Y-W 2004 Fracture of piezoelectromagnetic materials *Mech. Res. Commun.* **31** 65–73

Wang X and Pan E 2007 Magnetoelectric effects in multiferroic fibrous composite with imperfect interface *Phys. Rev.* B **76** 214107

Zheng J L, Fang Q H and Liu Y W 2007 A generalized screw dislocation interacting with interfacial cracks along a circular inhomogeneity in magnetoelectroelastic solids *Theor. Appl. Fract. Mech.* **47** 205–18